

## Equivalent permeability model for sealing evaluation of natural gas storage cavern in bedded rock salt

Tongtao Wang<sup>1,2</sup>, Chunhe Yang<sup>1,\*</sup>,  
Xiangzhen Yan<sup>2</sup>, Hongling Ma<sup>1</sup>, Xilin Shi<sup>1</sup>  
and J. J. K. Daemen<sup>3</sup>

<sup>1</sup>State Key Laboratory of Geomechanics and Geotechnical Engineering, Institute of Rock and Soil Mechanics, Chinese Academy of Sciences, Wuhan 430071, Hubei, China

<sup>2</sup>College of Pipeline and Civil Engineering, China University of Petroleum, Qingdao 266555, China

<sup>3</sup>Mackay School of Earth Sciences and Engineering, University of Nevada, Reno 89557, Nevada, USA

**An equivalent permeability model (EPM) is presented to calculate the equivalent permeability of non-salt layers, which makes the sealing evaluation of bedded salt cavern natural gas storage by numerical simulation easy and sufficient. In the numerical simulations, the effects of non-salt layer property parameters, i.e. horizontal permeability, vertical permeability and dip angle on the sealing of bedded salt cavern natural gas storage can be expressed by a single parameter, the equivalent permeability. We have studied the influence of non-salt dip angle, permeability anisotropy, permeability, buried depth, gas pressure, etc. on the time that it takes for the natural gas to migrate to the ground surface through the non-salt layer formation. The examples show that the EPM is precise and correct, and can meet the actual engineering demands, which includes fewer parameters, and it is implemented easily in numerical simulations. The time needed for natural gas to migrate to the surface is proportional to the increase in anisotropy of permeability and buried depth, but inversely proportional to the increase of non-salt layer dip angle, permeability and internal pressure. The permeability and the dip angle of non-salt layers are the key factors to be considered when analysing the sealing of bedded salt cavern natural gas storage.**

**Keywords:** Numerical simulation, permeability anisotropy, salt cavern, sealing.

ROCK salt, which has characteristic low permeability ( $10^{-20}$ – $10^{-22}$  m<sup>2</sup>), low porosity, damage recovery, favourable creep and easy solution in water, is considered as the most suitable type of formation to store oil, natural gas, radioactive waste, etc.<sup>1–5</sup>. For example, the British government has invested 0.93 billion dollars to construct more than 20 natural gas storage caverns in salt formation in 2010 and this has increased natural gas storage capacity by about 30% (ref. 6). During the design and sealing analysis of natural gas storage caverns, the rock salt is

suggested to be impermeable enough to fluid percolation on a geological time scale; however, the excavation disturbed zone (EDZ) with its increased permeability constitutes a potential path along which leakage of natural gas might occur<sup>7–10</sup>. Moreover, the permeability of non-salt layers in the bedded salt is much greater than that of rock salt<sup>5,11,12</sup>, which also increases the risk of leakage. In 1980, a leak occurred through corroded casing of a natural gas storage cavern in Barbers' Hill dome, Texas, and the natural gas likely moved through porous soil, which ultimately caused an explosion in a residence near Mont Belvieu<sup>13,14</sup>. Five years later, the leakage of natural gas caused another explosion and fire there again, which killed two people and prompted the evacuation of the entire town's population of more than 2000 residents. Therefore, sealing is one of the most important key indicators of natural gas storage cavern safety. In particular, for bedded salt cavern natural gas storages, if the appropriate measures and reasonable operating parameters are not taken, the natural gas could most likely migrate along the non-salt layers, faults and completion string channel (Figure 1) and potentially cause a disaster.

Many achievements have been made on the permeability tests of bedded salt and sealing evaluation of natural gas storage cavern according to available literature. For example, Hou<sup>8</sup> studied the effects of drilling on the permeability of rock salt in EDZ by laboratory experiments. The author found that the permeability of EDZ was about  $10^{-16}$  m<sup>2</sup> and decreased as the distance from the drilling hole increased. When the distance exceeded twice the hole diameter, it equalled that of the original salt, about  $10^{-21}$  m<sup>2</sup>. Results show that the disturbance produced by drilling has a significant influence on the permeability of rock salt. Deng *et al.*<sup>15</sup> obtained the air permeability of non-salt layer by testing more than 500 core samples from different strata and geological ages. Permeabilities ranged from  $5.50 \times 10^{-19}$  to  $6.94 \times 10^{-17}$  m<sup>2</sup>. They were

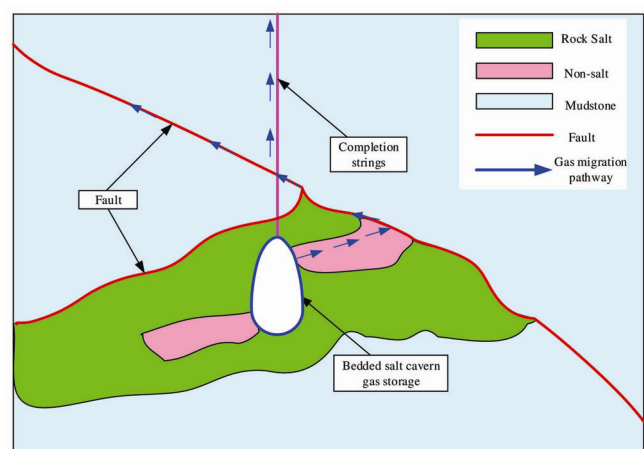


**Figure 1.** Natural gas migration pathway of a bedded salt cavern gas storage.

\*For correspondence. (e-mail: chyang@whrsm.ac.cn)

larger than that of rock salt by about 2 to 4 orders of magnitude under similar experimental conditions and exhibited anisotropy between the horizontal and vertical directions. Huang and Xiong<sup>16</sup> used the numerical simulations to study the tightness of salt cavern in Jintan salt mine of China, and demonstrated that the gas infiltration velocity along the damaged interface is much faster than the rock salt and mudstone interlayer, and the damaged interface is the main gas leakage path. Chen *et al.*<sup>17</sup> constructed an equivalent boundary gas seepage model to study the relation of gas seepage pressure and parameters of the contact face between salt and non-salt layers. The sealing of the West-1 and West-2 bedded salt cavern gas storages, located in Jiangsu province, China, was evaluated by the model; however, the effects of the dip angle, permeability magnitude, permeability anisotropy, cavern depth and gas pressure, etc., on the time it takes for natural gas to migrate to the surface were not discussed. Research results of these scholars show that the mechanical and physical properties of non-salt beds in bedded rock salt bear significant influences on salt cavern natural gas storage sealing.

The main objective of this communication is to develop an equivalent permeability model (EPM) to calculate the equivalent permeability of non-salt layers and then quantitatively assess the sealing of bedded salt cavern natural gas storage by numerical approaches. The sealing of a generic natural gas storage cavern in bedded salt is evaluated as an example, based on the model, by numerical simulations. The influence of the dip angle, permeability magnitude, permeability anisotropy, cavern depth and gas pressure on the sealing time of bedded salt cavern gas storage is studied. Encouraging results are obtained, which can provide examples and references for the design and monitoring of bedded salt cavern natural gas storage sealing.

Natural gas stored in a bedded salt cavern is likely to escape along the non-salt layers, as their permeability is much larger than that of rock salt<sup>16,18</sup>. The schematic of

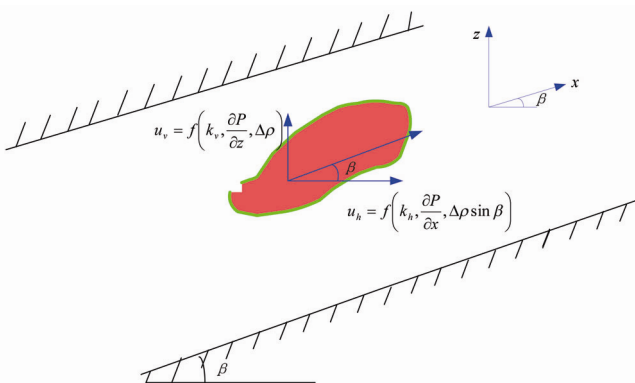


**Figure 2.** Schematic of natural gas migrating in a dipping non-salt layer.

natural gas migrating in a dipping non-salt layer is shown in Figure 2.

From Darcy's law, the natural gas and water flux speed in the dip direction are expressed as

$$u_{gx} = -\frac{k_h k_{rg}}{\mu_g} \left( \frac{\partial P_g}{\partial x} + \rho_g g \sin \beta \right), \quad (1)$$

$$u_{wx} = -\frac{k_h k_{rw}}{\mu_w} \left( \frac{\partial P_w}{\partial x} + \rho_w g \sin \beta \right). \quad (2)$$

Then, the migrating speed of natural gas along the vertical and horizontal directions in the dipping non-salt layer is written as

$$u_{gh} = \left( \frac{\lambda_{rg}}{\lambda_{rg} + \lambda_{rw}} \right) \left[ k_h k_{rw} \left( \Delta \rho g \sin \beta - \frac{\partial P_c}{\partial x} \right) \right], \quad (3)$$

$$u_{gv} = \left( \frac{\lambda_{rg}}{\lambda_{rg} + \lambda_{rw}} \right) \left[ k_v k_{rw} \left( \Delta \rho g - \frac{\partial P_c}{\partial z} \right) \right], \quad (4)$$

where  $u_{gx}$  and  $u_{wx}$  are natural gas and water migration speeds along the dip direction, respectively.  $k_h$  and  $k_v$  represent the absolute permeability of the non-salt layer along horizontal and vertical directions respectively.  $k_{rw}$  and  $k_{rg}$  stand for the relative permeability of natural gas and water.  $P_g$  and  $P_w$  are the pressure in natural gas and water phases respectively.  $\rho_g$  and  $\rho_w$  are the densities of natural gas and water phases respectively.  $\mu_s$  and  $\mu_w$  are the viscosities of natural gas and water phases respectively.  $\beta$  represents the dip angle of the non-salt layer.  $(\partial P_g / \partial x) = \nabla_x P_g$  is the pressure gradient in the gas phase in the dip direction.  $\lambda_{rg} = (k_{rg} / \mu_g)$  is the mobility of the gas phase.

The pathways of natural gas migrating in the non-salt layer along the horizontal and vertical directions are of distances  $l$  and  $h$  respectively, as shown in Figure 3 *a*. The EPM will be derived by equating the time it takes for natural gas to migrate the same vertical distance in the actual model (AM) and in the EPM.

As shown in Figure 3 *a*, the time taken by natural gas to migrate from A to B can be written as

$$t_h = \frac{l}{u_{gh}} = \frac{l}{\left( \frac{\lambda_{rg}}{\lambda_{rg} + \lambda_{rw}} \right) \left[ k_h \lambda_{rw} \left( \Delta \rho g \sin \beta - \frac{\partial P_c}{\partial x} \right) \right]}. \quad (5)$$

Similarly, the time taken by natural gas to migrate from B to C is

$$t_v = \frac{h}{u_{gv}} = \frac{h}{\left( \frac{\lambda_{rg}}{\lambda_{rg} + \lambda_{rw}} \right) \left[ k_v \lambda_{rw} \left( \Delta \rho g - \frac{\partial P_c}{\partial z} \right) \right]}. \quad (6)$$

Then, the total time for natural gas to migrate from A to C is  $t = t_h + t_v$ .

In EPM, we assume that the natural gas migrates only along the vertical direction, shown in Figure 3 b, and the permeability along the vertical direction is replaced by the equivalent permeability. Then, the migration speed of the natural gas is given by

$$u'_{gv} = \left( \frac{\lambda_{rg}}{\lambda_{rg} + \lambda_{rw}} \right) \left[ k'_v \lambda_{rw} \left( \Delta \rho g - \frac{\partial P_c}{\partial z} \right) \right]. \quad (7)$$

The time taken by natural gas to migrate the vertical distance  $h$  in the equivalent homogenous system is

$$t' = \frac{h}{u'_{gv}} = \frac{h}{\left( \frac{\lambda_{rg}}{\lambda_{rg} + \lambda_{rw}} \right) \left[ k'_v \lambda_{rw} \left( \Delta \rho g - \frac{\partial P_c}{\partial z} \right) \right]}. \quad (8)$$

Equating the time of the two models, we have

$$t' = t_h + t_v. \quad (9)$$

Substituting eqs (5)–(8) into eq. (9), the equivalent permeability is obtained as

$$k'_v = \frac{h}{l} \cdot \frac{1}{\left( \frac{k_v}{k_h} \right) \cdot \left( \frac{\Delta \rho g - (\partial P_c / \partial z)}{\Delta \rho g \sin \beta - (\partial P_c / \partial x)} \right) + 1} k_v, \quad (10)$$

where  $t_h$  and  $t_v$  are the times for the natural gas to migrate along the horizontal and vertical directions respectively.  $u'_{gv}$  represents the equivalent velocity.  $k'_v$  is the equivalent vertical permeability.  $t'$  is the time for natural gas to migrate in the equivalent model.

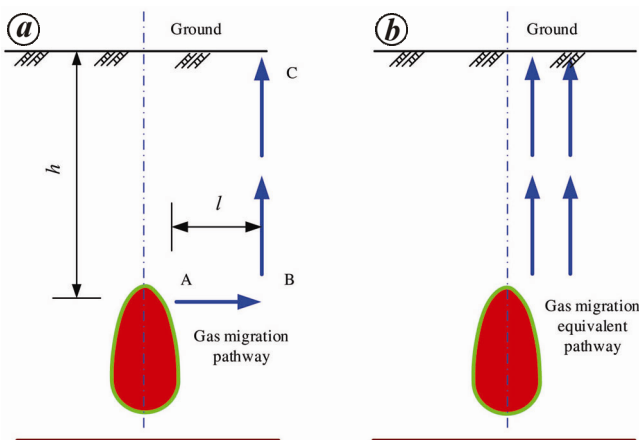


Figure 3. Equivalent Permeability Model of natural gas migrating from a bedded salt cavern gas storage.

From our analysis and explanation, we see that the main advantage of the EPM is that fewer parameters are included in the numerical simulation than in the AM, which makes the construction of the numerical model easier and improves the calculation efficiency. In the EPM, only one parameter, i.e. equivalent permeability, is needed to define the permeability of the non-salt layer; whereas for the AM there are three, viz. horizontal permeability, vertical permeability and dip angle. Here numerical approaches were used to closely simulate conditions similar to those that would be expected for a natural gas storage cavern to validate EPM and to study the effects of parameters on the sealing of bedded salt cavern natural gas storage. Figure 4 shows the assumed non-salt layer and geometry of the simulated generic salt cavern natural gas storage. The numerical simulations investigated several parameters: dip angle, permeability magnitude, permeability anisotropy, cavern depth and gas pressure. Equivalent permeability was calculated from the parameters of the AM by eq. (10), and used in the numerical calculations. The calculating precision and correctness of EPM were then evaluated by comparing its results obtained from the simulations and those of the AM.

The horizontal and vertical permeability of the non-salt layer are assumed equal, and assumed to be  $1 \times 10^{-17}$ ,  $1 \times 10^{-19}$  and  $1 \times 10^{-21} \text{ m}^2$  respectively. The numerical calculating time is for about 20 years. Results are shown in Figures 5–7.

Figure 5 shows the gas seepage pressure contour obtained by AM when the permeabilities of non-salt and rock salt layers are assigned as  $1 \times 10^{-17} \text{ m}^2$  and  $1 \times 10^{-19} \text{ m}^2$  respectively. It shows that gas gradually moves into the rock mass around the caverns with the

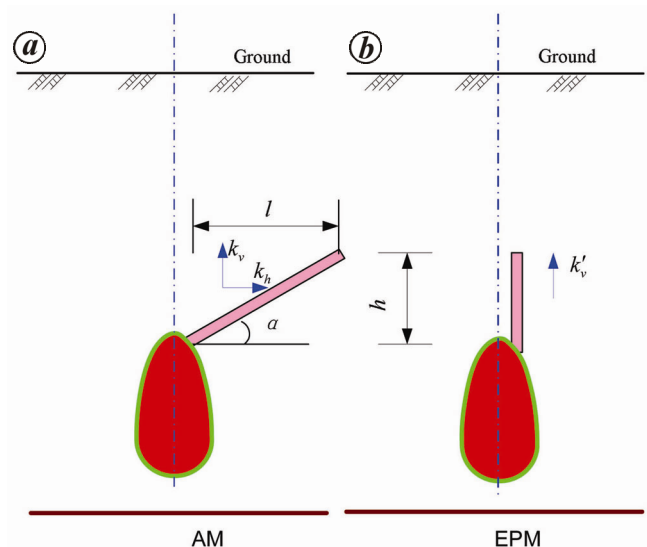
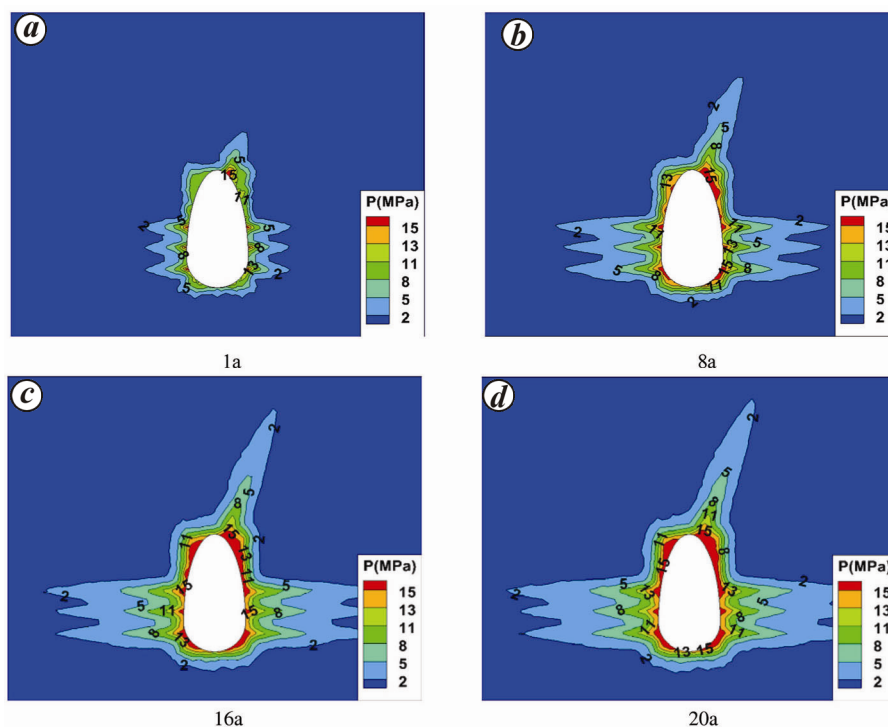
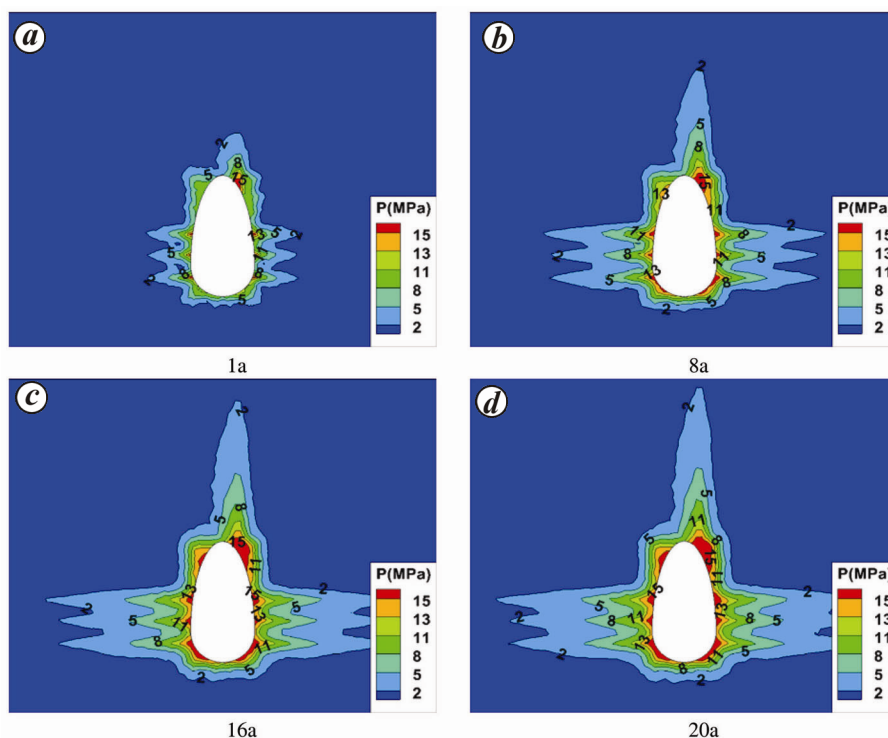


Figure 4. Sealing calculation schematic for a bedded salt cavern gas storage.



**Figure 5.** Gas seepage pressure contours obtained using the actual model when the permeabilities of non-salt and rock salt layers are assigned as  $1 \times 10^{-17} \text{ m}^2$  and  $1 \times 10^{-19} \text{ m}^2$  respectively.



**Figure 6.** Gas seepage pressure contours obtained using the equivalent permeability model.

increase of time. The migrating velocity of gas in the non-salt layer is larger than that in the rock salt. This is because the permeability of the non-salt layer is higher than that of the rock salt.

Figure 6 shows the gas seepage pressure contour obtained by EPM when the permeability of rock salt layers is assigned as  $1 \times 10^{-19} \text{ m}^2$  and the equivalent permeability of non-salt layer is calculated by eq. (10) based

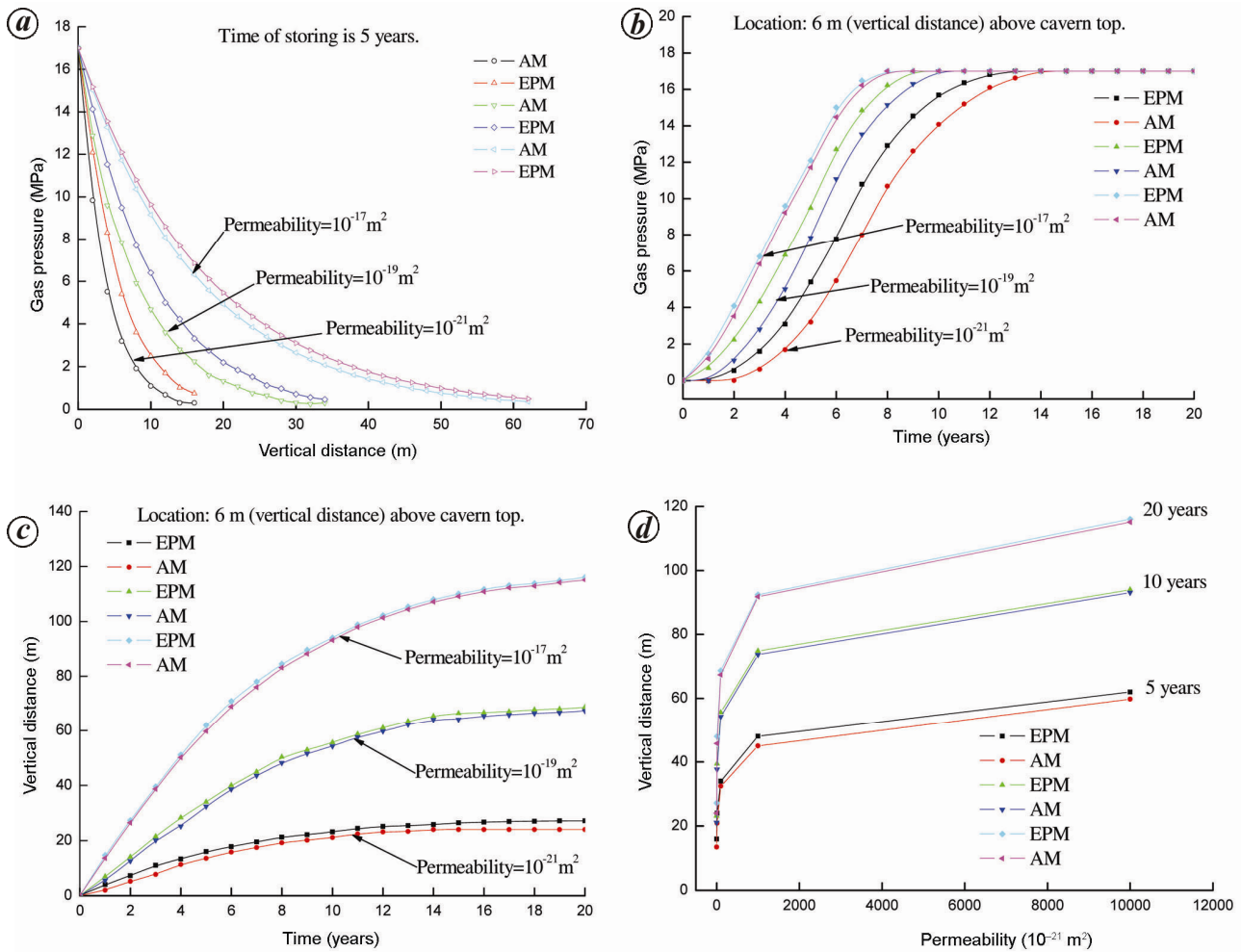


**Figure 7.** Results of the EPM and AM calculations when the dip angle of the non-salt layer is 20 degrees. *a*, Gas pressure versus vertical distance above the cavern top under different permeabilities of the non-salt layer. *b*, Gas pressure versus time under different permeabilities of the non-salt layer. *c*, Affected distance versus time for different permeabilities of the non-salt layer. *d*, Affected distance versus permeabilities of the non-salt layer at different times.

on the permeability used in AM. The migration of gas has similar characteristics as that obtained by AM.

Figure 7 shows the results of the two models obtained by the numerical simulations. As shown in Figure 7, the results of the EPM are well in accordance with those of the AM. The maximum differences of the gas pressure and effected distance obtained by the two models in the non-salt layer are less than 7% and 5% respectively. This indicates that the EPM has a high precision, and is correct, and can meet the actual engineering calculation demands. The gas pressure in the non-salt layer increases greatly as the permeability increases (Figure 7a). For example, the gas pressures at the location of 6 m (vertical direction) after a storing time of 5 years, are 5.40, 9.49 and 12.09 MPa when the values of permeability are  $1 \times 10^{-21}$ ,  $1 \times 10^{-19}$  and  $1 \times 10^{-17} \text{ m}^2$  respectively. As shown in Figure 7b and c, the gas pressure in the non-salt layer with high permeability increases rapidly and has a great extent. As the storage time increases, the affected distance increases and the penetration speed gradually

slows down. Numerical simulations also show that the differences between the results of EPM and AM grow as the permeability decreases. It is mainly because the distance that the gas infiltrates into EMP is bigger than that in the AM as shown in Figure 4, which causes the equivalent permeability to be larger than the original permeability based on eq. (10). The increase in permeability causes the effects of capillary porosity pressure on gas seepage velocity to decrease at the beginning, which makes a big difference in the results obtained by the two models. With increase of time, gas seepage trends become stable, and the effects of the capillary porosity pressure decrease. The errors in the results obtained by the two models decrease.

The examples in the previous paragraph show that EPM is precise and concise, and can be carried out easily by the numerical simulation with one parameter (equivalent permeability) to depict the gas flow in the non-salt layer. Therefore, EPM is used to study the effects of dip angle, permeability magnitude, permeability anisotropy,

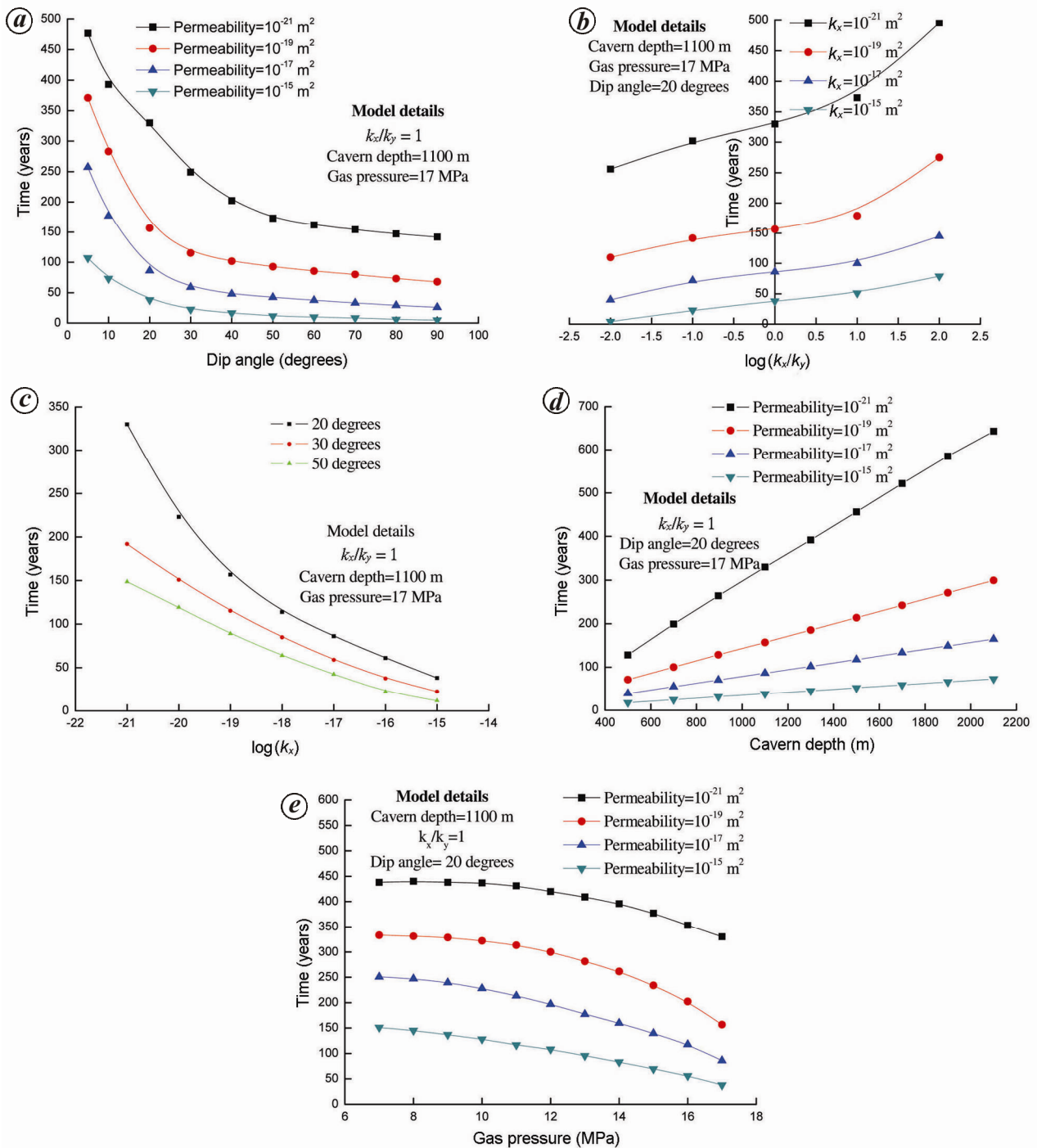


**Figure 8.** Influence of different parameters on the time required by natural gas to migrate from salt cavern to ground surface. *a*, Dip angle; *b*, Permeability anisotropy; *c*, Permeability; *d*, Cavern depth; *e*, Gas pressure.

cavern depth and gas pressure on the sealing of bedded salt cavern. The corresponding equivalent permeability is calculated by eq. (10), and used in the numerical model (Figure 4 *b*). The results are provided in Figure 8.

Figure 8 *a* illustrates the relation between the time taken by natural gas to migrate from the cavern to the ground surface and the dip angle under different permeabilities. The time decreases steeply as the dip angle

increases and gradually levels off. For example, when the permeability is  $10^{-15} \text{ m}^2$ , the time decreases from 73.06 to 22.4 years as the dip angle increases from  $10^\circ$  to  $30^\circ$ , a reduction of 69.34%. When the permeability is  $10^{-19} \text{ m}^2$ , the time is reduced by 59.23% under otherwise the same conditions. This indicates that the sealing of a bedded salt cavern with higher permeability non-salt layer is influenced more significantly by the dip angle. From eq. (10),

we find that the value of  $h/l$  increases dramatically with dip angle, which leads to an increase of equivalent permeability and a decrease of the resistance to gas migration. Ultimately, the time required by the gas to migrate to the surface and the leakage risk of bedded salt caverns increase. So, the dip angle and the permeability of non-salt layers are the key factors to be considered in the design to ensure the sealing of bedded salt cavern natural gas storage.

Figure 8b and c provides examples of the effects of permeability anisotropy and permeability magnitude on the sealing of bedded salt cavern natural gas storage. As shown in Figure 8b and c, the migration time increases with the value of  $k_x/k_y$  and decreases as the permeability increases. This reflects the fact that the vertical permeability of non-salt layer has more influence on the sealing than that of the horizontal direction. Small vertical permeability is good for the cavern sealing. Time has a linear relation with the cavern depth (Figure 8d) as it linearly increases the length of the natural gas leaking path. Figure 8e shows that high gas pressure has adverse effects on the sealing of bedded salt cavern natural gas storage, especially for caverns with high permeability non-salt layer, i.e. when the permeability is fixed as  $10^{-19} \text{ m}^2$ , the time required by natural gas to migrate to the surface reduces from 333 to 157 years as gas pressure increases from 7 to 17 MPa, a reduction of 53%.

The points discussed in this communication can be summarized as follows.

(i) An EPM is proposed to evaluate the sealing of natural gas storage caverns in bedded salt according to the characteristics of natural gas migrating in non-salt layers. Numerical models of generic bedded salt cavern natural gas storages are used to illustrate its advantages. The influences of several parameters on the bedded salt cavern sealing are studied, and quantitative relations are obtained.

(ii) Numerical simulations confirm that the results of EPM are precise, and the maximum differences between gas pressure and effected distance obtained by the EPM and AM in the non-salt layer are less than 7% and 5% respectively, which meets the engineering demands. The EPM includes fewer parameters and can be more easily carried out in numerical calculations than AM.

(iii) Results of the modelling effort show that the gas pressure and affected extent in the non-salt layer increase with time and permeability. The time taken by natural gas to migrate from a bedded salt cavern to the ground surface through a non-salt layer is proportional to the increase of permeability anisotropy, and cavern depth, but inversely proportional to the non-salt layer dip angle, permeability and internal pressure. Influences of dip angle, and permeability should be seriously considered during the design and site selection of bedded salt cavern gas storage to ensure cavern sealing.

1. Singh, T. N. and Verma, A. K., Prediction of creep characteristic of rock under varying environment. *Environ Geol.*, 2005, **48**(4/5), 559–568.
2. Yang, C. H., Li, Y. P., Qu, D. A., Cheng, F. and Yin, X. Y., Advances in researches of the mechanical behaviors of bedded salt rocks. *Adv. Mech.*, 2008, **38**(4), 484–494 (in Chinese).
3. Wang, T. T., Yan, X. Z., Yang, H. L., Yang, X. J., Jiang, T. T. and Zhao, S., A new shape design method of salt cavern used as underground gas storage. *Appl. Energy*, 2013, **104**, 50–61.
4. Bérest, P., Brouard, B., Mehdi, K. J. and Sambeek, L. V., Transient behavior of salt caverns – interpretation of mechanical integrity tests. *Int. J. Rock Mech. Min. Sci.*, 2007, **44**(5), 767–786.
5. Yang, C. H., Daemen, J. J. K. and Yin, J. H., Experimental investigation of creep behavior of salt rock. *Int. J. Rock Mech. Min. Sci.*, 1999, **36**(2), 233–242.
6. London looks underwater for gas storage; [http://www.upi.com/Business\\_News/Energy-Resources/2010/02/15/London-looks-underwater-for-gas-storage/UPI-63991266244162/](http://www.upi.com/Business_News/Energy-Resources/2010/02/15/London-looks-underwater-for-gas-storage/UPI-63991266244162/) (accessed on 1 January 2014).
7. Hakan, A., Percolation model for dilatancy-induced permeability of the excavation damaged zone in rock salt. *Int. J. Rock Mech. Min. Sci.*, 2009, **46**(4), 716–724.
8. Hou, Z. M., Mechanical and hydraulic behavior of rock salt in the excavation disturbed zone around underground facilities. *Int. J. Rock Mech. Min. Sci.*, 2003, **40**(5), 725–738.
9. Tsang, C. F., Bernier, F. and Davies, C., Geohydromechanical processes in the Excavation Damaged Zone in crystalline rock, rock salt, and indurated and plastic clays – in the context of radioactive waste disposal. *Int. J. Rock Mech. Min. Sci.*, 2005, **42**(1), 109–125.
10. Martino, J. B. and Chandler, N. A., Excavation-induced damage studies at the Underground Research Laboratory. *Int. J. Rock Mech. Min. Sci.*, 2004, **41**(8), 1413–1426.
11. Stormont, J. C., Conduct and interpretation of gas permeability measurements in rock salt. *Int. J. Rock Mech. Min. Sci.*, 1997, **34**(3–4), 303.e1–303.e11.
12. Pfeifle, T. W., Brodsky, N. S. and Munson, D. E., Experimental determination of the relationship between permeability and microfracture-induced damage in bedded salt. *Int. J. Rock Mech. Min. Sci.*, 1998, **35**(4–5), 593–594.
13. Thoms, R. L. and Gehle, R. M., A brief history of salt cavern use (keynote paper). In Proceedings of the 8th World Salt Symposium, (ed. Geertman, R. M.), Elsevier, 2000, pp. 207–214.
14. Evans, D. J., A review of underground fuel storage events and putting risk into perspective with other areas of the energy supply chain. *Geol. Soc. Spec. Publ., London*, 2009, **313**, 173–216.
15. Deng, Z. Y., Wang, S. C., Jiang, Z. L. and Chen, S. N., Breaking pressure of gas cap rocks. *Oil Gas Geol.*, 2000, **21**(2), 136–138 (in Chinese).
16. Huang, X. L. and Xiong, J., Numerical simulation of gas leakage in bedded salt rock storage cavern. *Proc. Eng.*, 2011, **12**, 254–259.
17. Chen, W. Z., Tan, X. J. and Wu, G. J., Research on gas seepage law in laminated salt rock gas storage. *Chinese J. Rock Mech. Eng.*, 2009, **28**(7), 1297–1304.
18. Yang, C. H., Li, Y. P., Chen, F. and Shi, X. L., Advances in researches of the mechanical behaviors of deep bedded salt rocks in China. In Proceedings of 43rd US Rock Mechanics Symposium and 4th US-Canada Rock Mechanics Symposium, American Rock Mechanics Association, Asheville, North Carolina, United States, 28 June–1 July 2009, ARMA-09-095.

ACKNOWLEDGEMENT. The authors acknowledge the financial support of National Natural Science Foundation of China (Grant Nos 41272391; 41472285; 51404241; 51304187; 51274187).

Received 25 February 2014; revised accepted 9 October 2014